The Ka-226 helicopter flight performance and its compliance with the modern requirements

B.A. Vassiliyev, V.N. Kvokov, F.N. Pavlidi, E.A. Petrosian, E.B. Feofilov

Kamov Company

Abstract

Presentation of Kamov Company activities aimed at provision of the Ka-226 helicopter flight performance compliance with the modern requirements, results of model and flight tests and their application in determination of the helicopter flight performance data in the whole range of expected operation conditions.

The multipurpose Ka-226 helicopter was developed by Kamov Company in 2003-2004 and certified in Category B and for operations using flight data of Category A.

The Ka-226 has a traditional Kamov coaxial design. The main rotors diameters are 13 m and the blades of each rotor are rectangular in form.

This article presents the main flight performance data of a Ka-226 helicopter model powered with Rolls-Royce 250-C20R engines. Materials of flight tests and analytical results were used.

The flight tests were performed in various conditions using several helicopters. The results of flight tests, ADT tests and test rig tests were used to refine the helicopter math models and to identify analytical programs with the purpose of determining the helicopter flight performance within the whole range of the expected operation conditions.

In the process of flight tests helicopter lift was evaluated many times at hover. **Fig. 1** presents the results of these tests that were performed at pressure altitudes to 350 m and outside air temperatures (OAT) of 4 to 17^{o}C. During the tests helicopter OGE hovers were performed at height 13-14 m over the ground. The maximum helicopter gross weight during the tests was 4050 kg, and the engine power was 884 hp. Calculations for ISA conditions and extrapolation of the test results in the considered conditions to engine take-off power provide the maximum helicopter lift of 4150 kgf. The helicopter thrust-to-weight ratio is 1.22 that is well acceptable for helicopters with a rotor load of 25-30 kgf/m^2.

Fig. 2 presents helicopter/rotor figure of merit versus rotor load ration $C_т/\sigma$ ($C_т$ - thrust coefficient, σ - rotor solidity ratio). It may be seen that the max helicopter figure of merit value obtained at tests was 0.714 and the rotor figure of merit value was 0.828 that answers the modern requirements. It must be noted that coaxial rotor configuration and absence of power losses for directional trimming (to 9-10 %) essentially increases the coaxial Ka-226 helicopter efficiency compared with single rotor helicopters.

High lift-to-drag ratio of the Ka-226 helicopter and its rotor can also be attributed to advanced TSAGI airfoils CTM and CTM2 used in the main rotor blades demonstrating high fineness. It is illustrated by **fig. 3** where results of CTM2 airfoil tests in TSAGI ADT -106 are presented in comparison with NACA 230 12 airfoil at Mach number 0.6 approaching the Ka-226 blade tip M value.

Fig. 4 presents flight test evaluations of the main rotor lifting capacity and validation of the rotor max lifting capacity limitations. Here max permissible rotor load $(C_T/\sigma)_{perm}$ is presented versus relative speed (relation of helicopter speed to rotor blade tip peripheral velocity) in straight flight conditions and in steady and transient maneuvers. These graphs were obtained based on experimental and analytical data. Some experimental points are marked on the graphs as highlights. Additional flight test checks of the rotor max lifting capacity in straight flight allowed to expand the limitations in these conditions. This dependence is used to calculate the max permissible helicopter speed. Besides, this dependence is used in the helicopter Air Data System for determination of the max allowable helicopter speed, and its indication by a movable index and warning system in the cockpit.

Fig. 5 presets the helicopter rate of climb at take-off and cruise engine ratings, helicopter hover and service ceilings, max and min helicopter speeds versus pressure altitude. The highlighted points mark results obtained in flight tests made to check the flight data and limitations. The checks were performed within the range between the max and min permissible IAS values (red stars). The max permissible IAS was checked with an excess of 40 km/h (to 250 km/h). The rate of climb and service ceiling were checked to an altitude of 3500 m, that is, to the altitude limit value established for the helicopter without oxygen breathing equipment on board. In max speed check flights OAT temperatures ranged within –5.5 to +26°C, in flights at min speed it was –25 to +26°C and in flights to check the rate of climb and service ceiling – 3 to +22°C. In the course of flight limitation checks all required measurements were taken; control margins, specific parameters of the power plant operation, structural component loads and blade approach limits were determined that demonstrated flight safety in the helicopter operational flight range.

An important problem of a safe flight provision is evaluation of trimming characteristics in flight tests and provision of adequate control margins in the whole range of operational flight conditions.

Fig. 6 presents results of flight test evaluation of control travels in various steady flight conditions in the range of extreme c.g. positions:

- in level flight at speeds ranging from 40 km/h in backward flight to max forward speed of 210 km/h;
- in flights near ground in various directions;
- in flights with slip angles to ±30 градусов;
- in conditions of climb, motor gliding and autorotation.

The test results show that adequate control margins are available in operation flight conditions. It is also demonstrated that the helicopter complies with the modern requirements for max tail/side wind speed values that must not exceed 9 m/s. The data presented illustrates also the coaxial helicopter aerodynamic symmetry. It may be seen that in flight conditions without slipping (red marks) the cyclic travels practically along the axis of symmetry and the positions of the pedals are near the neutral. The cyclic and pedals move to the right and left mainly when slipping is there and in sideward flights from hover.

In the course of tests control margins were also tested at banked turns, ascending and descending spirals with ±45 degs bank, various unsteady maneuvers like accelerations and decelerations, roll reversals within ±55-60 degs, reversals from one slipping angle to another within ±30 degs, transfers to climb and descent, zooms.

Flight evaluation proved that the selected control parameters ensure excellent helicopter control parameters and harmonious helicopter control.

Fig. 7 presents the main results of static stability evaluation obtained at flight tests. Compliance with the longitudinal stability versus helicopter speed requirements were demonstrated by a trade-off selection of the stabilizer (elevator) installation angle that provided for adequate control margins and the required level of static stability. As an example, fig. 7 presents longitudinal control stick travel versus helicopter speed obtained in compliance with the standard requirements at a constant collective pitch value in level flight conditions at a speed near to cruise and within the operational c.g. position range.

It may be seen that the stick speed gradient is positive that indicates to the availability of longitudinal static stability versus speed.

In the course of final development activities helicopter directional static stability performance was improved. For that purpose the data obtained in flight tests of the Ka-226 prototypes (helicopters Ka-26 and Ka-126), ADT tests using Ka-26, Ka-126 and Ka-226 helicopter models were used. Flight and model tests showed that modification of the Ka-126 and Ka-226 helicopter airframe aerodynamic configuration as compared to the Ka-26 resulted in reduction of directional static

stability versus slipping angle and consequently led to the change of pedal travel gradient versus slipping angle when performing steady slipping maneuvers.

In order to improve the level of directional static stability certain measures were taken.

Special slats were designed, installed on the helicopter vertical stabilizers and flight tested Ka-126 helicopter and Ka-226 helicopter model. It should be noted that similar slats were first installed on the Ka-27 and Ka-32 helicopters and their versions. These slats allowed to increase the stabilizer lifting capacity at large slipping angles. The slats designed for the Ka-226 and installed on its vertical stabilizers were expected not only to increase the lifting capacity but also to improve the helicopter directional static stability. To do that, it was decided to increase considerably the relative square area of the slats (i.e. the ratio of the slat square area to the stabilizer square area). Tests of the Ka-226 model in TSAGI T-102 ADT demonstrated high effectiveness of this configuration and flight tests performed first on the Ka-126 and later on the Ka-226 confirmed the effectiveness of the slats.

Results of the Ka-226 flight tests showed that besides installation of slats some other measures are required in order to improve the directional static stability versus slipping angle. ADT tests of various model variants revealed that the optimal approach is to increase the tail section “arm” by lengthening the helicopter tail booms. A trade-off decision was taken to increase the length of tail booms by 350 mm. **Fig. 7** presents results of flight tests undertaken to evaluate the level of helicopter directional static stability with tail booms of initial and increased (by 350 mm) length at 160 km/h. It can be seen the with initial tail boom length the helicopter was practically neutral as regards the slip angle and practically did not comply with the standard requirements at the given speed but acquired considerable directional static stability after extension of the booms. The requirements on directional static stability are complied with in all conditions indicated in the norms.

Fig. 8 presents variation of helicopter flight parameters (roll/pitch angles, pedal travel, angular rates) in left/right rotations at hover. It may be seen that with the pedal traveling to the stop the rate of rotation for 2.5 s reached 60 ^{o}/s and continued to increase (recording equipment range was limited to ±60 ^{o}/s). The helicopter motion was stopped by pressing the other pedal for approximately the same time of 2.5 s. The bank increased to 10 degs to one or the other side and the pitch angle changed insignificantly.

A series of analytical and experimental evaluations of the Ka-226 helicopter take-off and landing performance were performed at Kamov involving establishment of normal take-off/ landing trajectories and procedures (in conditions of the powerplant normal operation) and demonstration of compliance with Category A requirement for safe continued and aborted take-off and safe

continued and aborted landing OEI. Based on the results of these tests recommendations were drawn up for introduction n the helicopter Flight Manual.

Fig. 9-14 shows variation of flight parameters for a helicopter of 3400 kg take-off weight flying the above procedures.

Fig. 9-10 presents time variation of flight parameters at aborted take-off based on flight test data. Engine failure was simulated at height 15 m and V≈65 km/h (fig. 9). After the engine failure the main rotor speed demonstrates a short-term decrease to 95%. The vertical speed decreases and the helicopter transfers to a descent at 2.5 to 3 m/s. At deceleration the vertical speed drops to 0.5 m/s at the touch down moment. The vertical overload at the moment of touch down is 1.6g. Aborted take-off trajectory and distance were calculated based on flight test data. It may be seen that the trajectory is located beyond the H-V zone (fig. 10) and an aborted take-off distance here is around 300 m.

Fig. 11-12 presents time variation of flight parameters at OEI landing. The engine failure was simulated at approximately height 90 m and V≈85 km/h. After the engine failure the main rotor speed demonstrates a short-term decrease to 97%. The vertical speed increases to 5 m/s and at deceleration the vertical speed drops to 0 m/s at the touch down moment. The vertical overload at the moment of touch down was 1.9g. OEI landing trajectory and distance were calculated based on the flight test data. It may be seen that the trajectory is located beyond the H-V zone (fig. 12), the landing speed is 20 km/h and a landing distance from height 15 m to the touch down here is approximately 60 m.

Fig. 13 presents examples of continued take-off and aborted landing conditions flown at tests. Here variations of radio altimeter altitude, IAS and pitch angle versus time are presented. The points of engine failure simulation at take-off and landing are marked down. The presented data illustrates continued take-off and aborted landing performance. An engine failure was simulated in continued take-off at height 12 m and V≈70 km/h. A permitted increased torque engine rating was used for 16 s. That considerably improves transient conditions after engine failure and allows to accelerate after the engine failure to $V=V_Y$ (the best climb speed value) without descent and even with climb continuation. The main rotor speed demonstrates here a short-term decrease and the gas temperature do not exceed 800 ^oC that is quite acceptable. The transient conditions presented in fig. 13 were maintained within 15 s. After termination of transient conditions the pilot reduces the engine rating to 30 min. OEI and the climb is continued at this rating till $V = V_Y$ is attained with a climb rate of 1 m/s. Utilization of transient conditions and high efficiency of the coaxial Ka-226 helicopter ensure continued take-off and climb without any drop of height during one engine failure simulation.

In aborted landing simulation an engine failure was simulated at height 25 m and V=80 km/h. After normalized delay of 1 s the pilot accelerated to $V = V_Y$ and transferred to climb at this speed. The

loss of height was around 10 m but the helicopter did not go down below the prescribed height 10.7 m. It may be seen that the aborted landing is a more complicated maneuver because here it is required to transfer from descent to climb. Presented materials show that it is provided for on the Ka-226 helicopter and after transient conditions the helicopter continues to climb practically along the same trajectory as when performing continued take-off.

So the tests demonstrated that for take-off the decision point height of **12 m** and helicopter speed of **60 km/h** in this point can be accepted. At landing the height of decision point of **25 m** and helicopter speed of **80 km/h** are accepted.

The flight test results, absence of altitude drop after simulation of an engine failure in flight at take-off show, that it is possible to reduce the height of the take-off decision point to 3 m. In this case it is necessary to accelerate more aggressively in order to attain the speed of 60 km/h by instrument at this height. **Fig. 14** presents realizations of helicopter continued take-off at the max take-off weight and different take-off decision point height values (12 m and 3 m). It may be seen that after simulation of en engine failure at height 3 m the helicopter power potential is enough to ensure continued take-off in compliance with the requirements. Moreover, the helicopter is capable to perform a continued take-off without an altitude drop. Reduction of height at the decision point at take-off allows to reduce from 260 to 125 m the horizontal distance covered by the aircraft with respect to the ground surface to the moment the V_{TOSS} (safe take-off speed for Cat A rotorcraft) is reached as well as an aborted take-off distance. That considerably expands the helicopter operational capabilities.

Aviation rules demand demonstration of an autorotation landing capability. A procedure of helicopter landing at autorotation was developed and test pilots made such landings with simulation of both engine failure. When developing and testing the procedure, Kamov used its experience in testing of coaxial helicopters and results of numerical experiments.

Fig. 15 presents time variation of flight parameters experienced in one of autorotation landings. Landing approach was made at V= 80 km/h. Flaring was made at height 12-14 m by increasing the pitch angle along with attaining helicopter landing attitude at height 3-4 m. Aggressive pull up by collective was performed at height 3-4 m. Landing speed was around 30 to 40 km/h (speed indictor was beyond the sensitivity zone), vertical overload at the moment of landing did not exceed the allowable level of 2.5g. According to pilot comments, the helicopter controllability in the process of autorotation and landing maneuvers was acceptable and a safe landing was ensured.

Fig. 16 presents results of flight tests aimed at evaluation of the helicopter rate of climb in OEI flight at 30 min power (OEI) and vertical decent speed at autorotation. Analytical data is also presented.

Flights with one engine inoperative were performed in the altitude range of 0 to 500 m, at OAT of 15 to 20 ^{o}C and at 3400 kg helicopter weight. The calculations were performed for ISA conditions, pressure altitude of 300 m. The presented results show that in the examined conditions the Ka-226 helicopter max rate of climb OEI at 30 min power occurs at 90-00 km/h and is equal to 1-1,2 m/s. Steady rate of climb value 0.5 m/s is attained at 70-75 km/h (steady safe speed value).

Autorotation fight tests were performed at gross weights of 3100 to 3400 kg, pressure altitudes to 2800 and OAT range –6 to +18 ^{o}C. Autorotation conditions were attained by putting the throttles in Low Idle position when the engines torques were zeroed. Fig. 16 presents autorotation descent vertical speed versus IAS in test conditions. Calculations are presented for ISA, pressure altitude of 1000 m. It can be seen that the minimum vertical descent speeds of 7-8 m/s occur at IAS = 75-85 km/h. With the helicopter speed decrease or increase the descent speed increases. Helicopter controllability was also evaluates at autorotation tests. The flight tests showed that autorotation control margins are adequate and the helicopter possesses acceptable controllability characteristics. Efficient rudders are installed in the Ka-226, as well as on its prototypes that ensure directional control. Installation of slats on the vertical fins enhances the efficiency of the rudders.

Conclusion

- Characteristics of the Ka-226 helicopter powered with Rolls-Royce engines 250-C20R obtained in flight tests and based on numerical model and calculations are presented.

- The Ka-226 helicopter flight performance fully complies with the modern requirements for the helicopters of this class. The helicopter flight performance complies with the Category A requirements of the Aviation Rules.

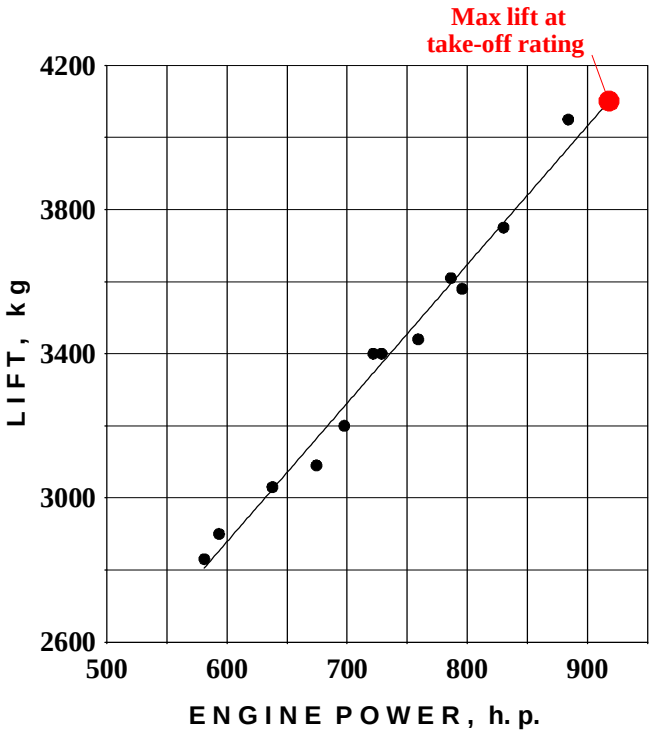

Fig. 1. Ka-226 helicopter lift evaluation flight data

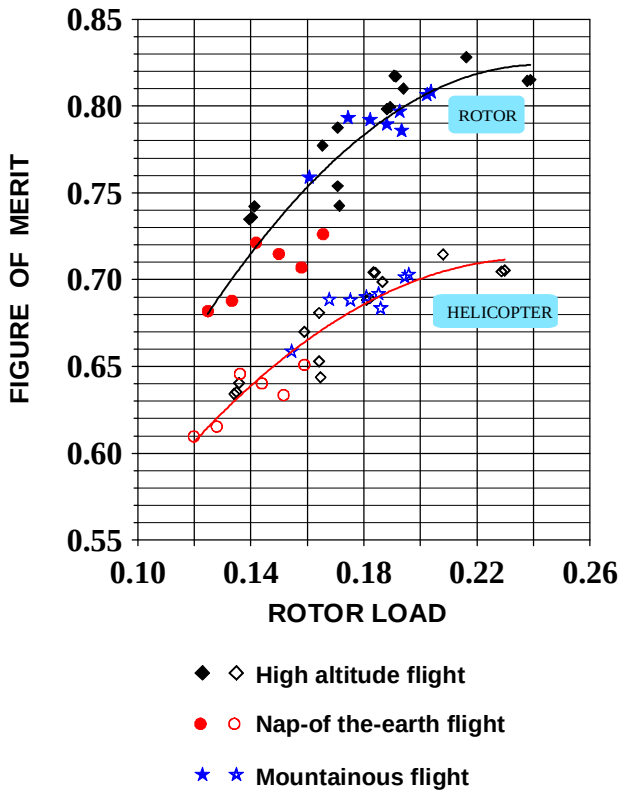

Fig. 2. Helicopter/main rotor figure of merit versus rotor load based on flight test data

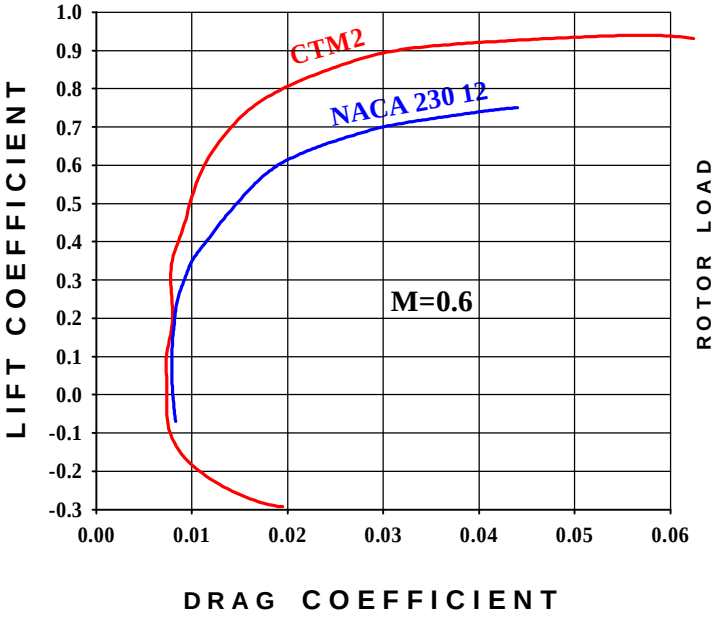

Fig. 3. CTM2 and NACA 230 12 airfoil profile polars based on ADT test data

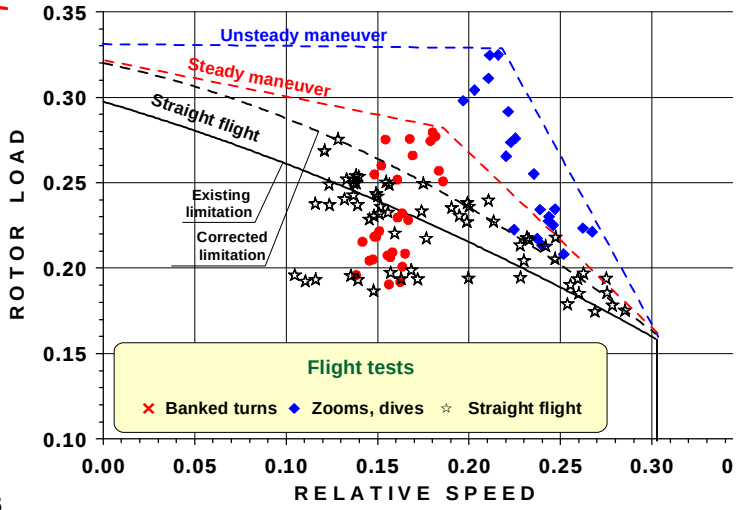

Fig. 4. Rotor carrying capacity

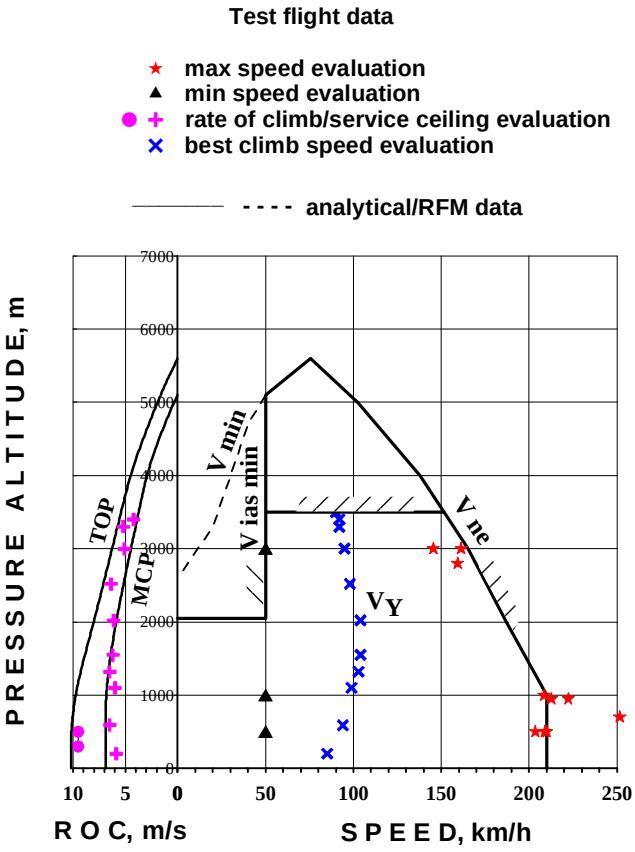

Fig. 5. Max/min speeds, rate of climb, service/hover ceiling values

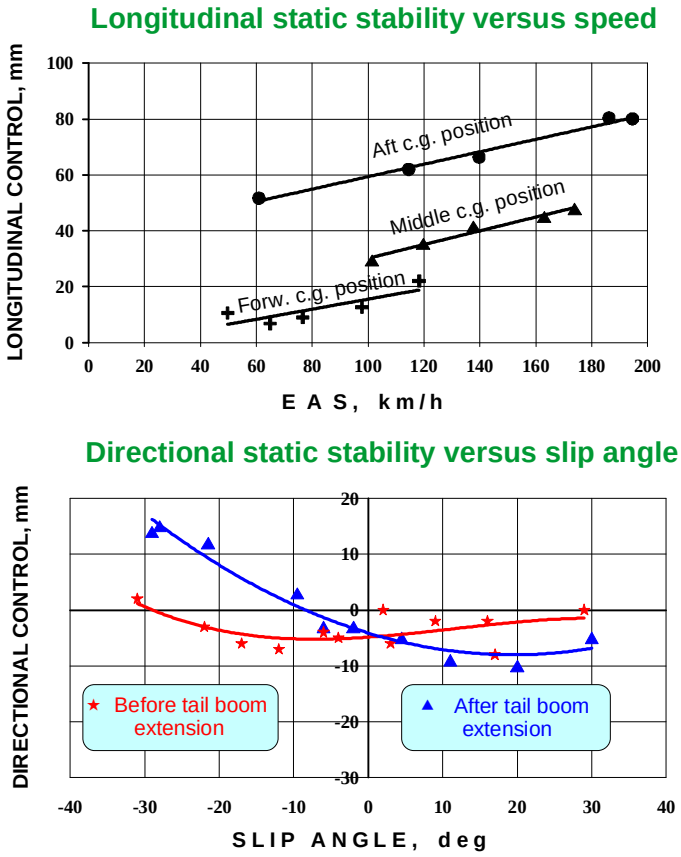

Fig. 7. Flight test data. Static stability

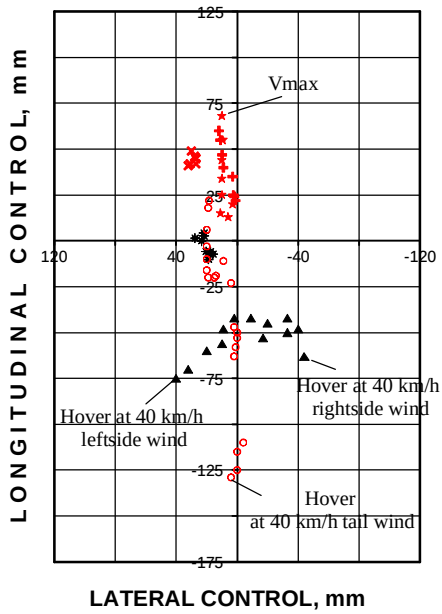

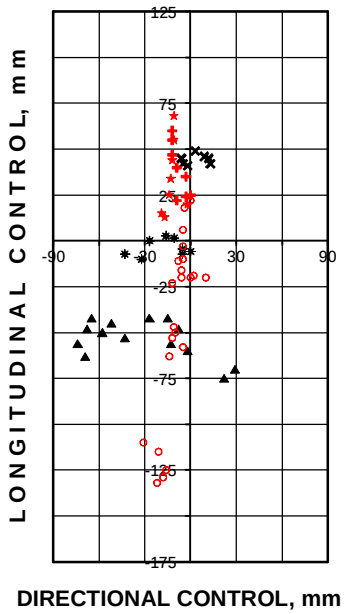

- Flight near ground, extreme forward c.g. position
- Level flight, extreme aft c.g. position
- Climb at take-off rating, extreme aft c.g. position
- Autorotation, extreme forward c.g. position
- Flight near ground leftwards/rightwards from hover (hover at wind from right and left), forward c.g. position
- Slipping to 30 deg. angles from level flight at IAS=160 km/h, middle c.g. position

Fig. 6. Control margins

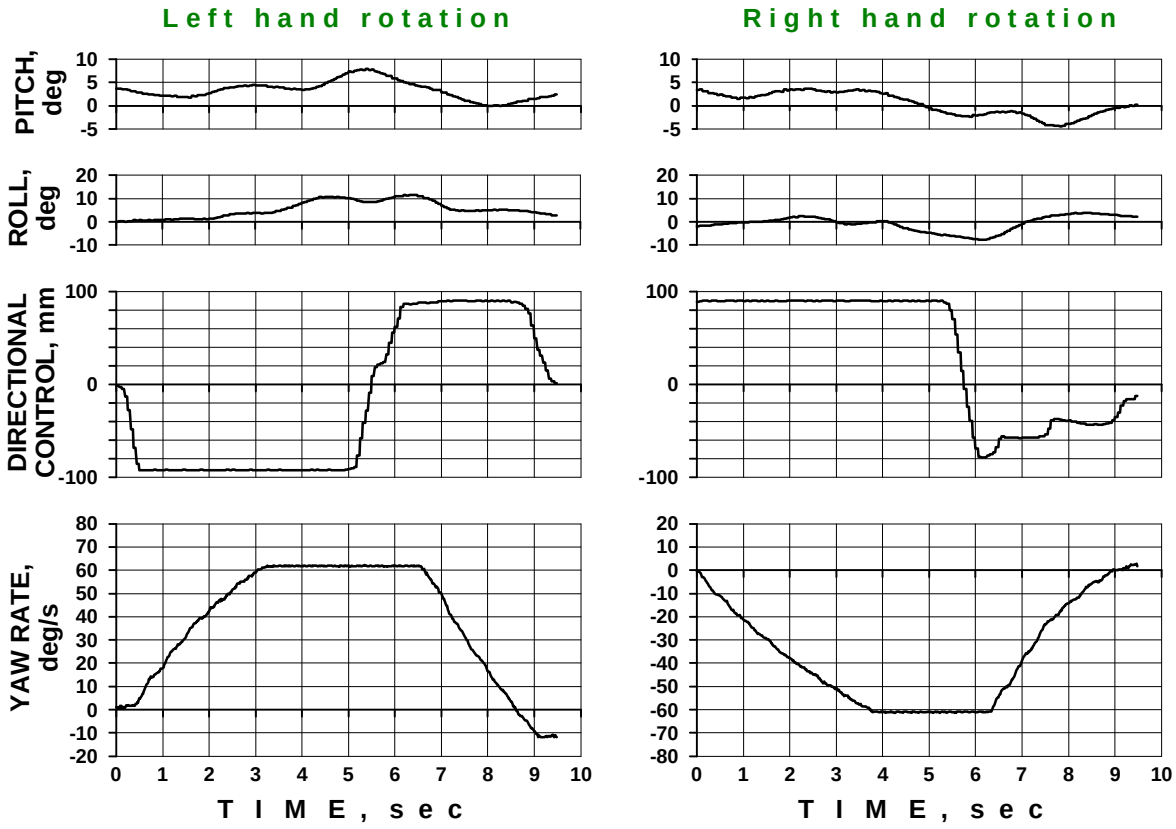

Fig. 8. Flight tests. Helicopter flight parameter variations at max take-off weight when performing hover turns

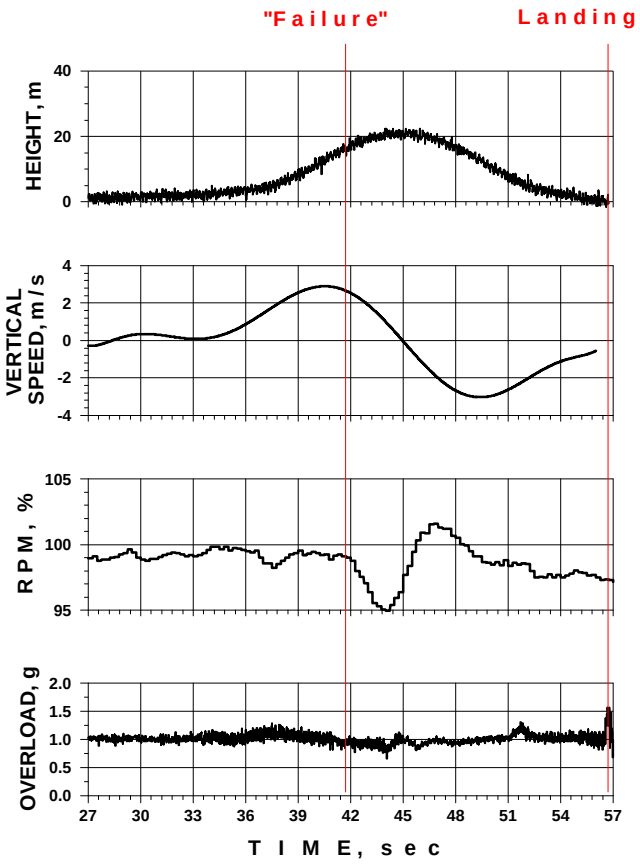

Fig. 9. Flight tests
Time variations of helicopter motion parameters in aborted take-off conditions. Weight 3400 kg

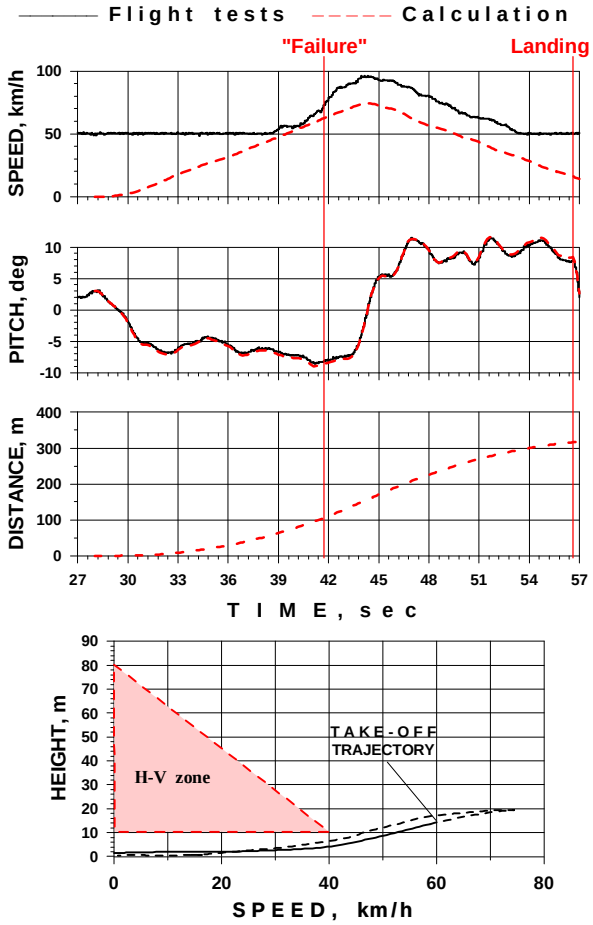

Fig. 10. Restoration of aborted take-off parameters based on test flight data

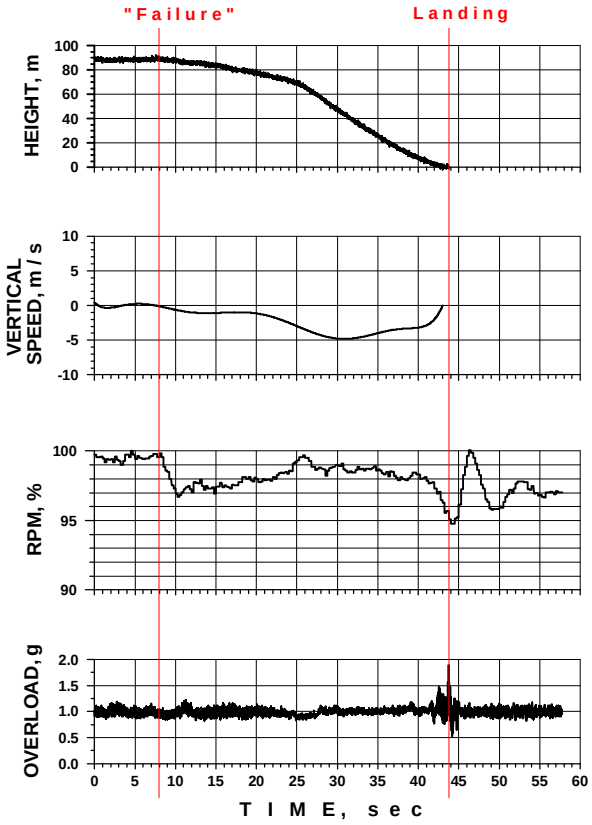

Fig. 11. Flight tests
Time variations of helicopter motion parameters in OEI landing conditions. Weight 3400 kg

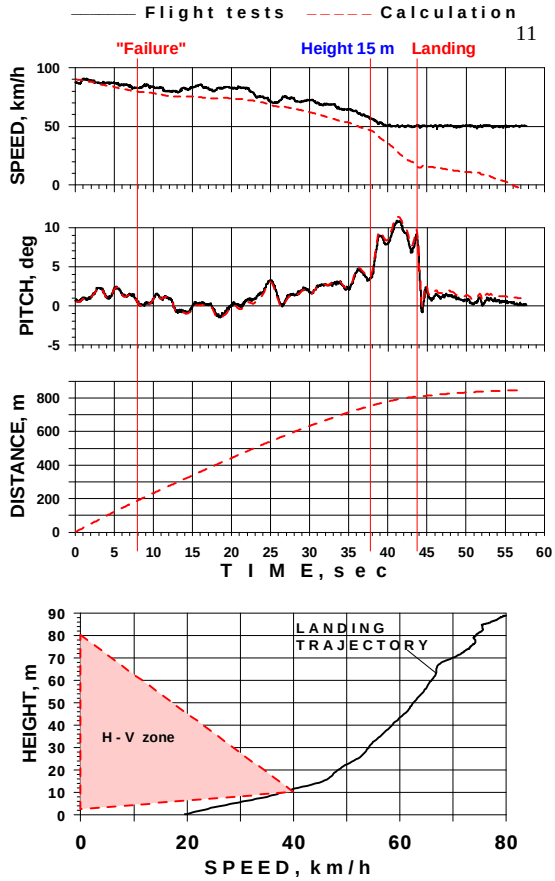

Fig. 12. Restoration of OEI landing parameters based on test flight data

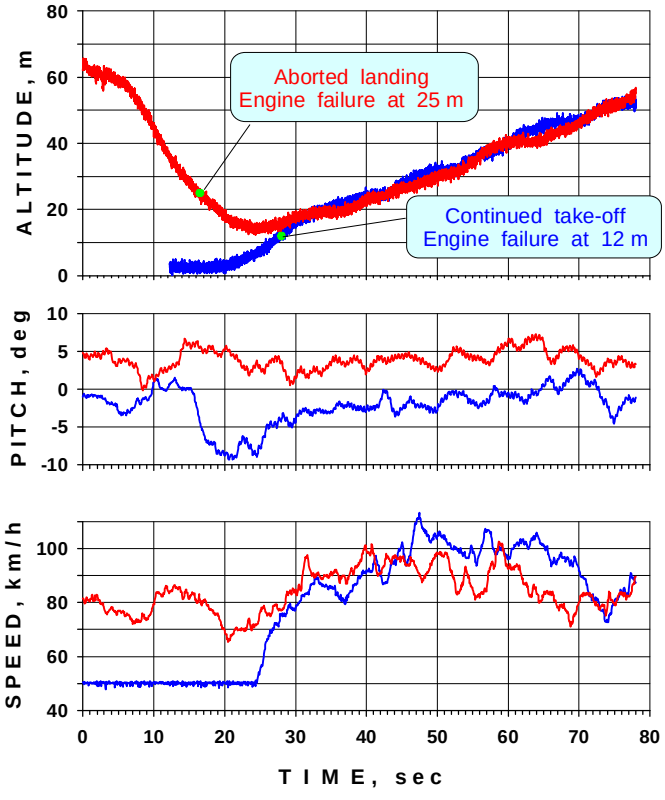

Fig. 13. Flight tests. Weight 3400 kg
Time variations of helicopter motion parameters in continued take-off and aborted landing conditions.

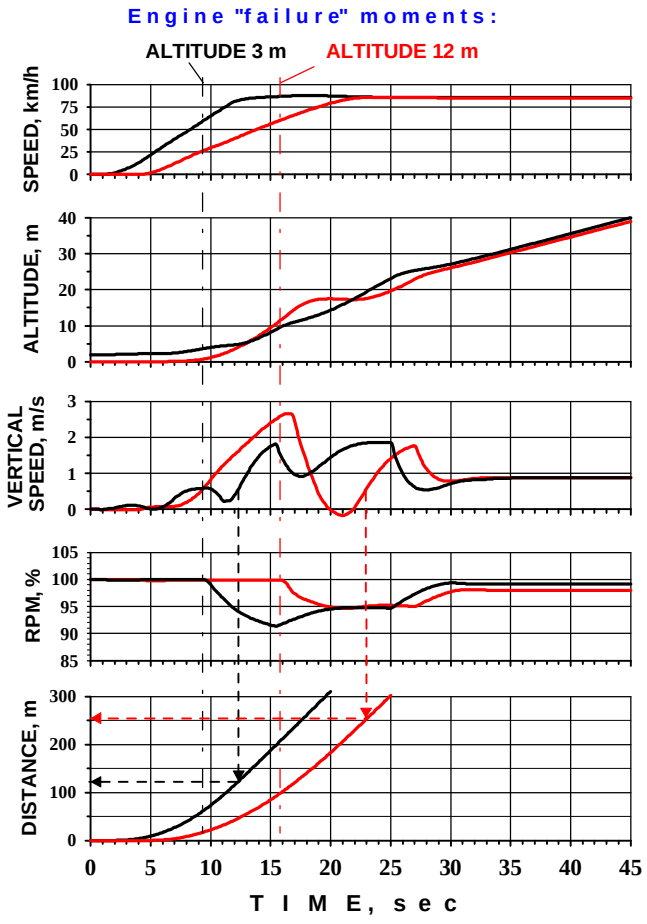

Fig. 14. Numerical experiment. Variations of helicopter motion parameters in case of one engine "failure" at various altitudes

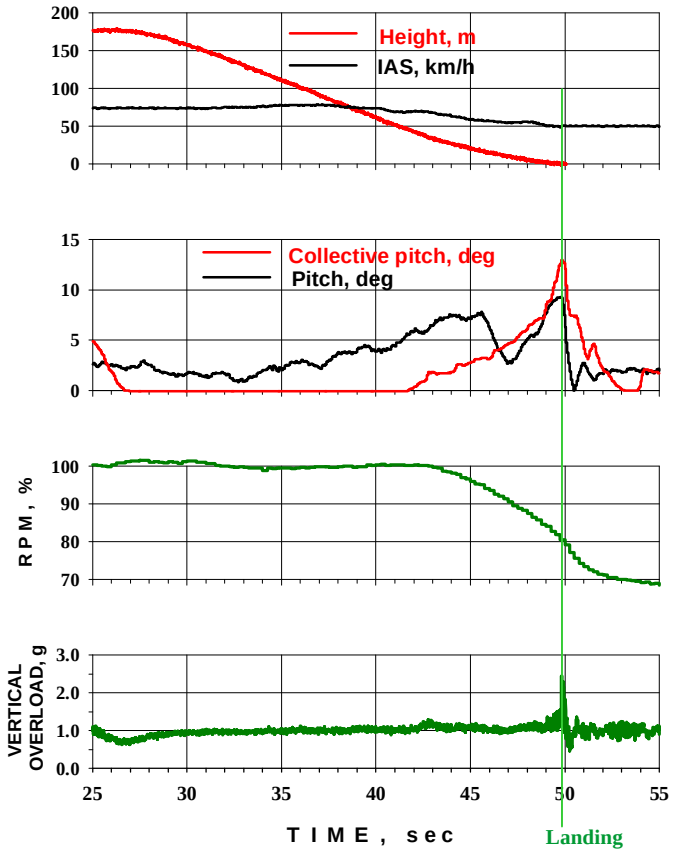

Fig. 15. Flight tests
Time variations of helicopter motion parameters in autorotation landing conditions with maximum weight

Vertical speed in OEI flight

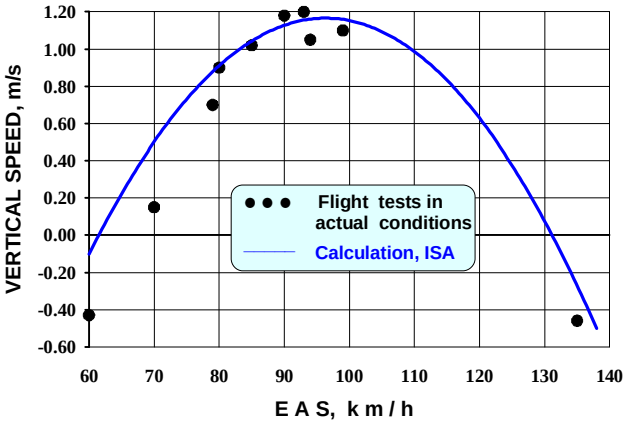

Vertical descent speed in autorotation conditions

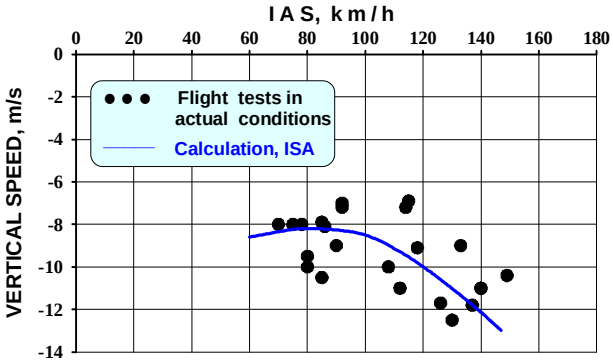

Fig. 16